Supplement of Atmos. Meas. Tech., 12, 1935–1954, 2019
https://doi.org/10.5194/amt-12-1935-2019-supplement

Atmospheric Measurement Techniques
Open Access

*Supplement of*

# Chemical ionization quadrupole mass spectrometer with an electrical discharge ion source for atmospheric trace gas measurement

**Philipp G. Eger et al.**

*Correspondence to:* John N. Crowley (john.crowley@mpic.de)

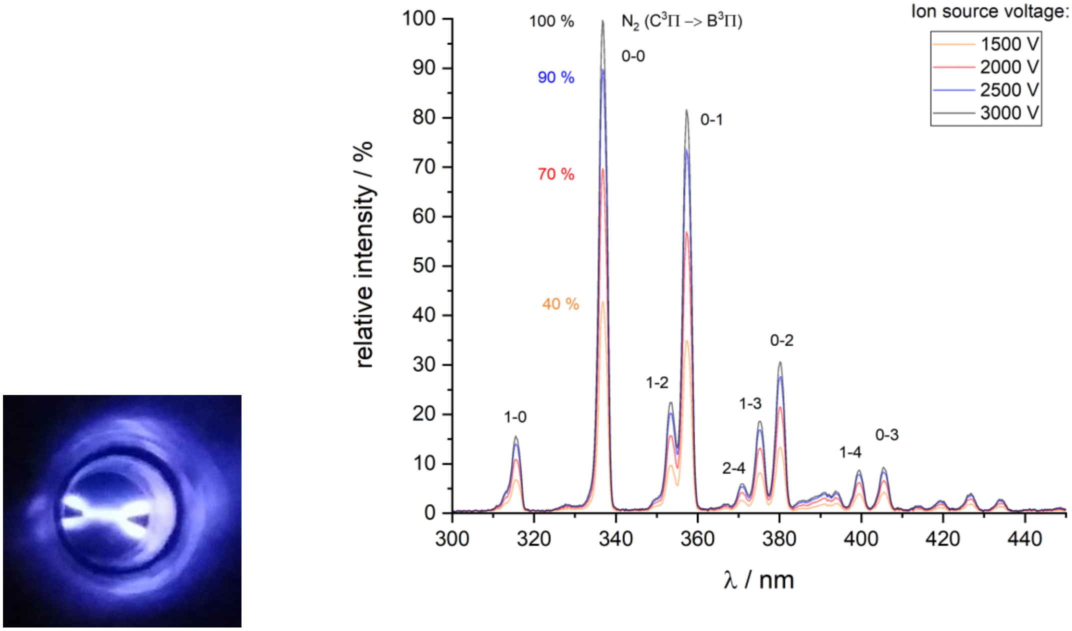

**Figure S1**. Photo: $N_2$ emission observed between and around the pointed tungsten tips of the electrodes of the RF discharge source. Right: The emission spectrum was recorded with an Ocean-Optics USB-4000 spectrometer with optical fibre at various high-voltages. The strongest features (not fully resolved using the low-resolution ($\Delta\lambda \approx 1.5$ nm) spectrograph) can be assigned to transitions from the ground vibrational level of the electronically excited $N_2$ ($C^3\Pi_u$) state to the $B^3\Pi_g$ state.

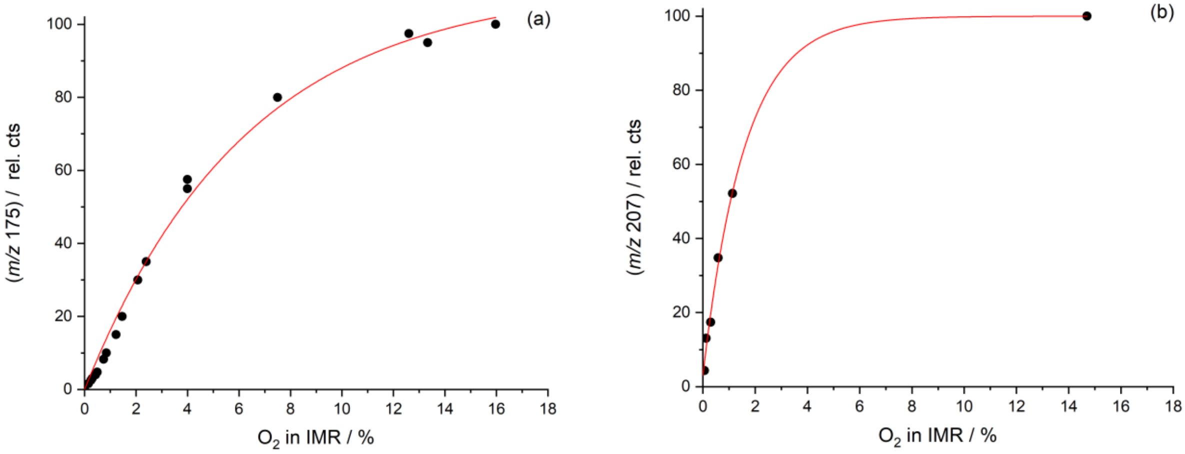

**Figure S2**. (a): Dependence of $IO_3^-$ signal (*m/z* 175) on the fractional pressure of $O_2$ in the IMR when adding 800 sccm $N_2$ / $CH_3I$ through the RF discharge region. (b): Signal at *m/z* 207 ($ISO_3^-$) for a constant amount of $SO_2$ over the same range of $O_2$ partial pressures.

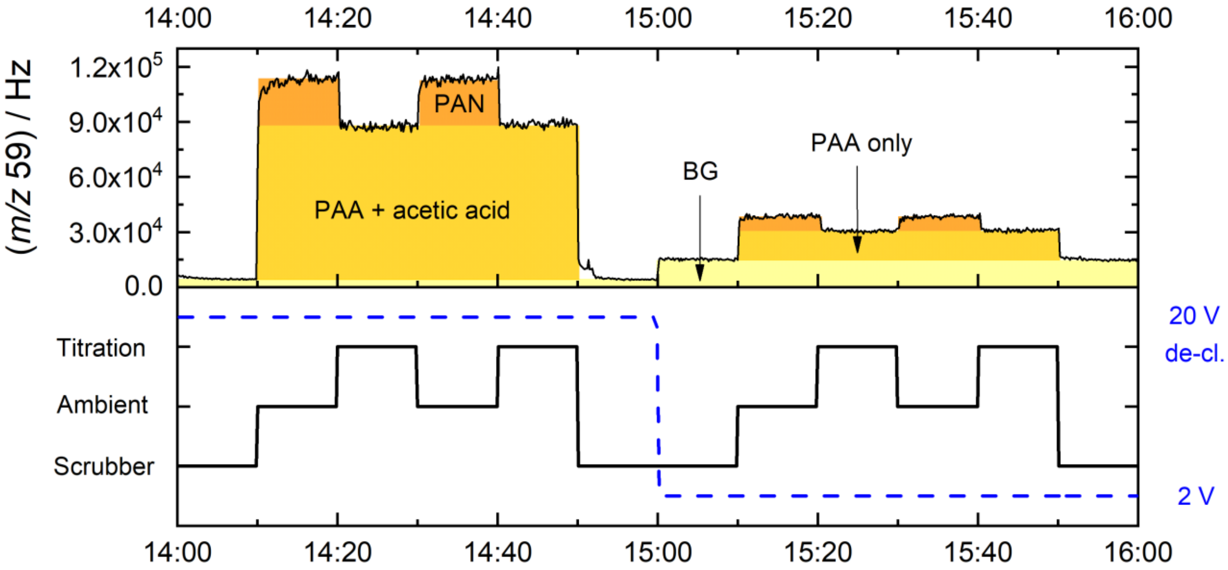

**Figure S3**. Exemplary time series of the CI-QMS signal at *m/z* 59 when sampling from the photochemical PAN calibration source described in Sect. 2.7. The instrument periodically switches between the states “scrubber”, “ambient” and “titration” (i.e. addition of NO). In ambient mode we measure the total signal of PAN, PAA and acetic acid. When adding NO to the inlet, the peroxyacyl radicals are titrated and the signal consists of PAA and acetic acid only. Changing the de-clustering voltage (at 15:00) from 20 V to 2 V results in the complete loss of sensitivity for acetic acid. During measurements of ambient air, the de-clustering voltage is usually changed more frequently, which means for each data point we firstly measure the signal at *m/z* 59 with high de-clustering and immediately afterwards with low de-clustering.

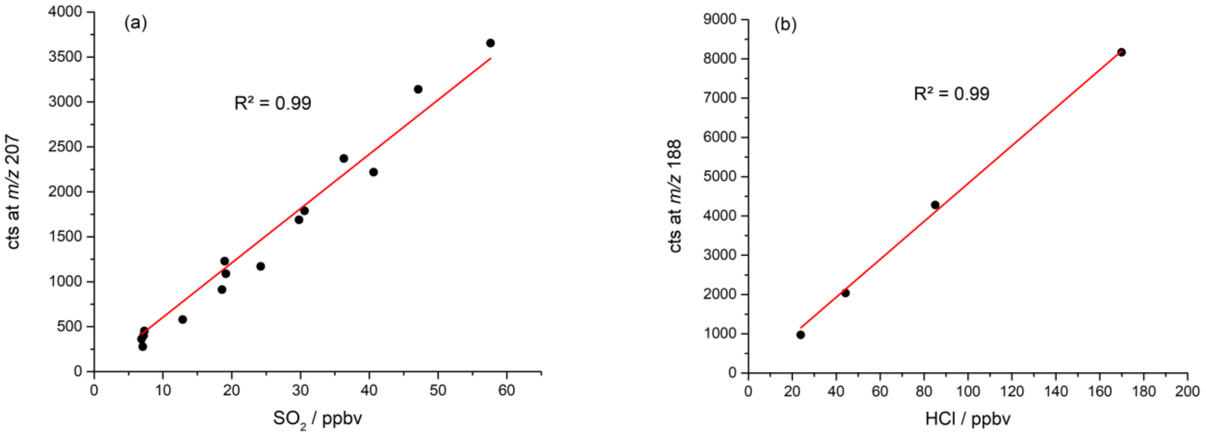

**Figure S4**. (a) Linear dependence of count rate at *m/z* 207 ($ISO_3^-$) on the $SO_2$ mixing ratio of the sample measured. (b) Linear dependence of count rate at *m/z* 188 ($I(CN)Cl^-$) on the HCl mixing ratio.

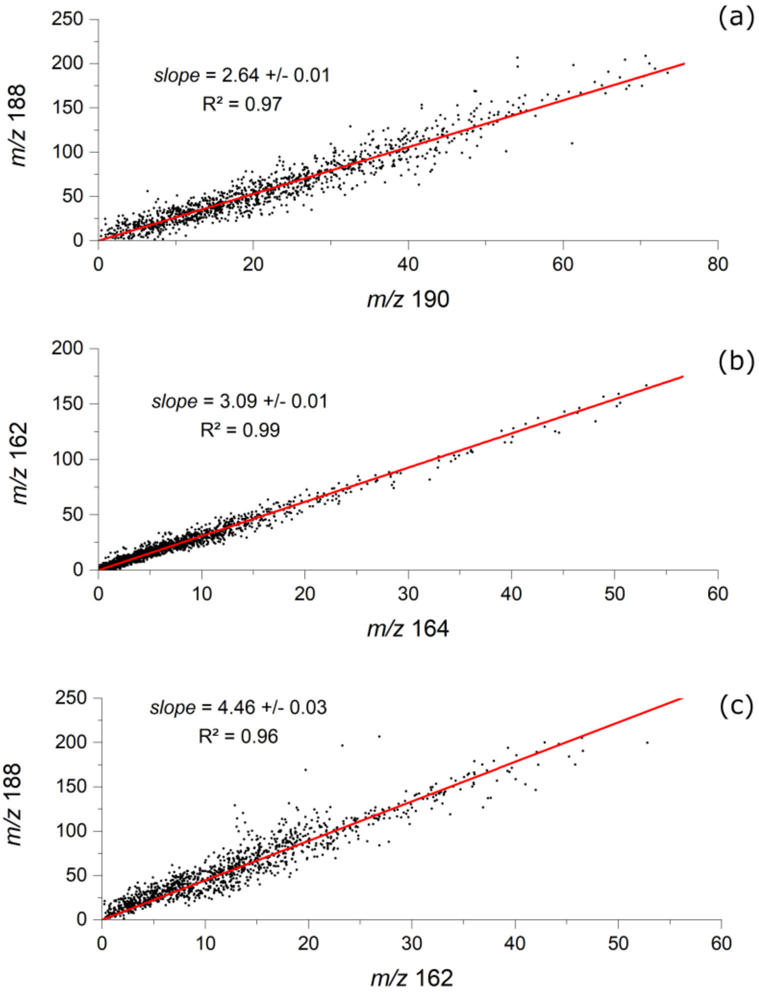

**Figure S5**. (a) and (b): Correlation of ion signals at *m/z* 162 versus *m/z* 164 ($ICl^-$) and *m/z* 188 versus *m/z* 190 ($I(CN)Cl^-$) during CYPHEX. The expected slope resulting from the isotopic abundance of $^{35}Cl$ to $^{37}Cl$ is 3.13. (c) Signal at *m/z* 188 versus *m/z* 162. The linear correlation indicates that both ions are from the same trace gas, HCl.

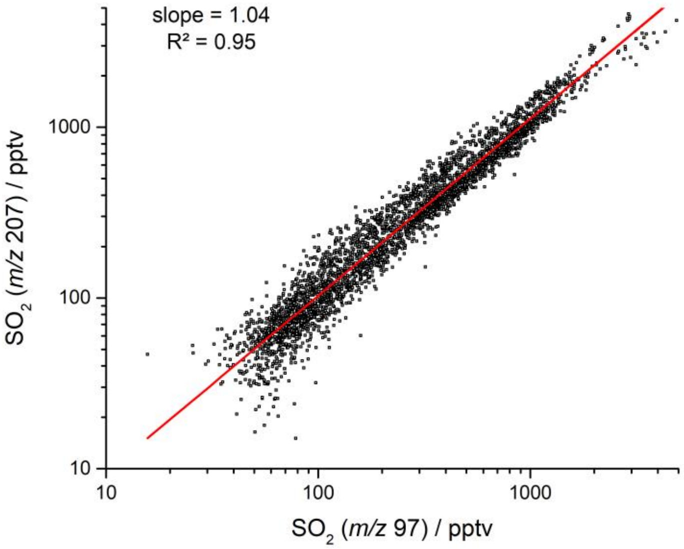

**Figure S6:** Correlation between the CI-QMS measurement of $SO_2$ at *m/z* 207 ($ISO_3^-$) vs. *m/z* 97 ($HSO_4^-$) during NOTOMO.

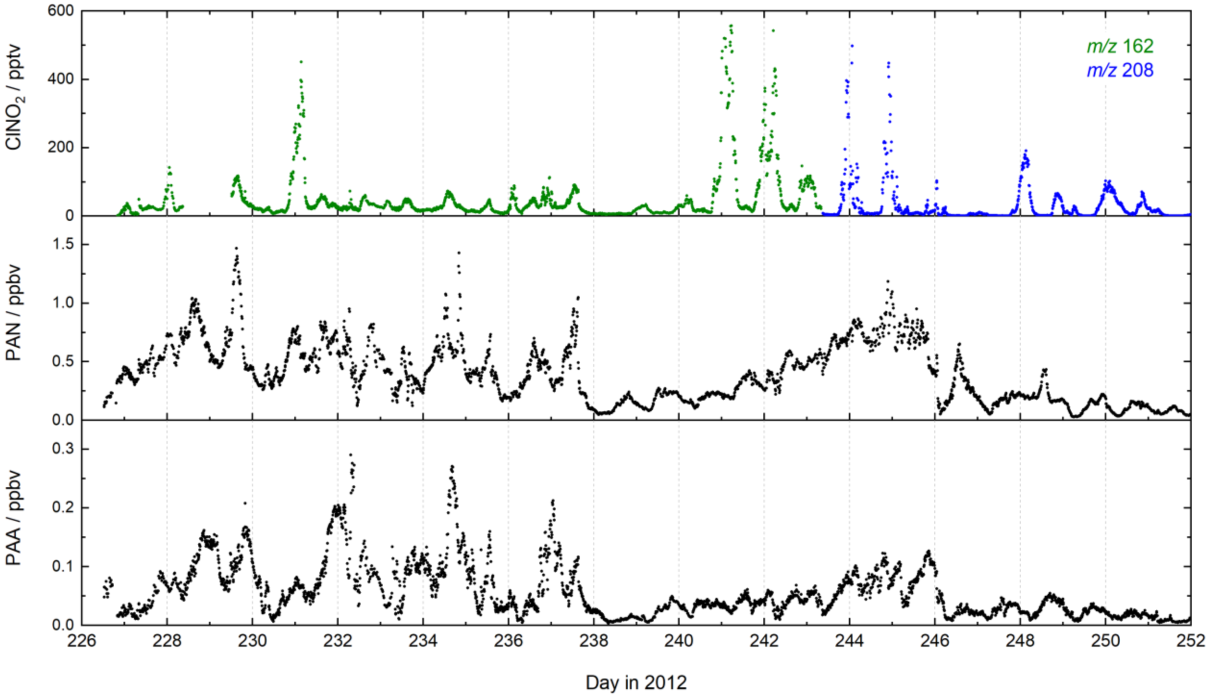

**Figure S7:** Measurements of ClNO$_2$, PAN and PAA using CI-QMS with a $^{210}$Po-ionisation source during the PARADE campaign, which took place at the same location and similar time of year as the NOTOMO campaign in which the RF discharge was deployed. The ClNO$_2$ data during PARADE has been reported by Phillips et al. (2012).